

Research Article

# Marine Sponge *Xestospongia* sp.: A Promising Source for Tuberculosis Drug Development - Computational Insights into Mycobactin Biosynthesis Inhibition

Arfan <sup>1\*</sup>   

Aiyi Asnawi <sup>2</sup>  

La Ode Aman <sup>3</sup>  

<sup>1</sup> Department of Pharmacy, Universitas Halu Oleo, Kendari, Southeast Sulawesi, Indonesia

<sup>2</sup> Department of Pharmacy, Universitas Bhakti Kencana, Bandung, West Java, Indonesia

<sup>3</sup> Department of Pharmacy, Universitas Negeri Gorontalo, Gorontalo, Gorontalo, Indonesia

\*email: [arfan09@uho.ac.id](mailto:arfan09@uho.ac.id); phone: +6285340837856

## Keywords:

Docking  
Molecular dynamics  
*Mycobacterium tuberculosis*  
Mycobactin  
Salicylate synthase  
*Xestospongia* sp.

## Abstract

*Mycobacterium tuberculosis* (MTB) remains the leading cause of infection, with a significant fatality rate, owing primarily to drug resistance. MTB contains the enzyme salicylate synthase, which regulates mycobactin production to bind iron ions from the host cell, facilitating the bacteria to grow and reproduce. This study investigates the potential of marine sponges to inhibit the MTB salicylate synthase by exploiting a computational approach combining molecular docking and dynamics simulations. Forty-six compounds from *Xestospongia* sp. were chosen from the Marine Natural Products database. The docking results selected four compounds (CMNPD15071, CMNPD7640, CMNPD26706, and CMNPD7639) from this sponge, which provide more negative binding energy than their inhibitors (RVE). After reclassifying their interactions, such as hydrophobic and hydrogen bonds, CMNPD15071 (Sulfuric acid mono-(8-methoxy-12b-methyl-6-oxo-2,3,6,12b-tetrahydro-1H-5-oxa-benzo[k]acephenanthrylen-11-yl) ester) and CMNPD7640 (secoadociaquinone B) performed molecular dynamics simulations to assess their stability. These two compounds show a promising stability profile compared to RVE based on RMSD, RMSF, SASA, and gyration analysis. Furthermore, the binding affinity prediction of these two compounds using the MM/GBSA calculation method reveals that CMNPD15071 (-38.48 kJ/mol) had the highest affinity for binding to MTB salicylate synthase compared to RVE (-35.36 kJ/mol) and CMNPD7640 (-26.03 kJ/mol). These findings demonstrate that compounds from *Xestospongia* sp. can block MTB mycobactin biosynthesis by inhibiting salicylate synthase.

Received: July 28<sup>th</sup>, 2023

1<sup>st</sup> Revised: January 25<sup>th</sup>, 2024

Accepted: February 13<sup>th</sup>, 2024

Published: February 29<sup>th</sup>, 2024



© 2024 Arfan, Aiyi Asnawi, La Ode Aman. Published by Institute for Research and Community Services Universitas Muhammadiyah Palangkaraya. This is an Open Access article under the CC-BY-SA License (<http://creativecommons.org/licenses/by-sa/4.0/>). DOI: <https://doi.org/10.33084/bjop.v7i1.5513>

## INTRODUCTION

Mycobacterium is a worldwide endemic bacterium involving non-pathogenic and pathogenic species associated with infection in many organisms, especially humans and animals<sup>1,2</sup>. *Mycobacterium tuberculosis* (MTB) is a respiratory infection thought to infect one-quarter of the world's population, and as a bacteria, it has killed more individuals than any other in human history<sup>3</sup>. Around 10.6 million tuberculosis (TB) cases will occur in 2021, with up to 1.6 million people dying globally<sup>4,5</sup>. Tuberculosis therapy is still a challenge, in part due to drug resistance<sup>6</sup>. As a response, discovering and developing drugs to overcome this disease remains urgently needed<sup>7</sup>. Salicylate synthase from MTB is one of the most appealing targets for developing and identifying new anti-TB drugs<sup>8</sup>.

Salicylic synthase is responsible for the biosynthesis of mycobactin MTB by converting chorismate to salicylic acid<sup>9</sup>. Mycobactin is a small molecule (siderophore) synthesized by MTB that binds iron ions from host proteins such as transferrin

**How to cite:** Arfan, Asnawi A, Aman LO. Genetic CYP2A6 Marine Sponge *Xestospongia* sp.: A Promising Source for Tuberculosis Drug Development - Computational Insights into Mycobactin Biosynthesis Inhibition. *Borneo J Pharm.* 2024;7(1):40-50. doi:10.33084/bjop.v7i1.5513

and lactoferrin. MTB requires iron ions to replicate hence inhibiting salicylate synthase activity in mycobactin production is a promising target for anti-TB drugs<sup>10,11</sup>. In addition, mycobactin is not present in host cells, so inhibiting this enzyme can be a potential drug target<sup>12</sup>. A recent study revealed the potential for inhibition of MTB salicylate synthase by 5-phenylfuran-2-carboxylate and chromane derivatives with inhibition concentrations (IC<sub>50</sub>) of 250 μM and 55 μM, respectively<sup>13,14</sup>. However, due to a lack of information on inhibitors of this enzyme, the search for compounds that can inhibit salicylate synthase from MTB is still essential, particularly those derived from natural sources.

The marine is a natural resource with high biodiversity and rich in active chemicals spread in various marine ecosystems and can be developed into medicine<sup>15,16</sup>. Marine natural resources such as mollusks, algae, and sponges offer a high potential for development as pharmaceutical raw materials<sup>17</sup>. *Xestospongia sp.* is a species of sponge that has been shown to have anti-inflammatory, antioxidant, antibacterial, antifungal, antiviral, and anticancer activities<sup>18</sup>. Because the activity of *Xestospongia sp.* against MTB is still relatively limited, this investigation was conducted to explore and study the anti-TB activity of bioactive compounds from *Xestospongia sp.* molecularly utilizing a computational study approach. This research is also expected to obtain the lead compounds as inhibitors of the salicylate synthase enzyme from MTB.

## MATERIALS AND METHODS

### Materials

#### Enzyme structures

The structure of MTB salicylate synthase (PDB ID: 3ST6) crystallized with native ligand (RVE) was considered due to its high resolution (1.75 Å) (<https://www.rcsb.org/>)<sup>19</sup>. The crystallographic structure was created by omitting the protein's B, C, and D chains and the associated residues, such as water molecules, to verify the quality of the docking procedure<sup>20</sup>. Lastly, polar hydrogen atoms and Kollman charges were adjusted to the target protein using AutoDock Tools v.1.5.6<sup>21</sup>.

#### Test compounds structures

Forty-six *Xestospongia sp.* compounds were collected from the Comprehensive Marine Natural Products Database (<https://www.cmnnpd.org/>)<sup>22</sup>. The test compounds were selected based on the 400-500 g/mol molecular weight range. All test compounds' structures were converted into \*pdbqt format using Open Babel<sup>23</sup>. Bound inhibitor (RVE) was employed as a control to compare with the test compounds.

### Methods

#### Molecular docking study

Molecular docking was performed using Autodock software to determine the binding affinity and interactions between compounds from *Xestospongia sp.* against MTB salicylate synthase<sup>24</sup>. The docking process was confirmed to the enzyme binding site using the redocking method by calculating the root mean square deviation (RMSD) of the RVE conformation, which must be less than 2 Å<sup>25</sup>. The test compounds were docked following the RVE binding coordinates with a cubic conformational search area of 40 Å. The docking technique involves the Genetic Algorithm, performed up to 100 times run. The population was limited to 150, with a maximum of 2,500,000 number evaluations. The other docking algorithm and parameters were left as default settings.

#### Enzyme-compound interactions analysis

The best compound's conformation from the docking process was continued to the interaction analysis stage. Discovery Studio Visualizer v17.2.0.16349 software was used to study and depict hydrogen bonds and hydrophobic interactions produced between enzymes and the best compounds.

#### Molecular dynamics simulation

Molecular dynamics (MD) simulations were carried out using the GROMACS 2022 package<sup>26</sup>. Protein topology was prepared using AMBER99SB-ILDN<sup>27</sup>, and ligand topology was designed using the General AMBER Force Field (GAFF)<sup>28</sup> generated with the help of ACPYPE<sup>29</sup>. This simulation was carried out in an aqueous environment as a cubic box using the TIP3P water molecule model. The neutral system was obtained after adding Na<sup>+</sup> and Cl<sup>-</sup> ions<sup>30,31</sup>. An equilibrium system

consisting of protein, ligand, solvent, and ions was received after simulating NVT and NPT at 300 K with a pressure of 1 bar<sup>32</sup>. The production system lasts for 50 ns. The simulation results were analyzed using the RMSD, root mean square fluctuation (RMSF), solvent accessible surface area (SASA), and radius of gyration (Rg) criteria. Lastly, the binding affinity was calculated using the MM/GBSA method approach.

### Data analysis

For molecular docking, the RMSD value was calculated by measuring the distance of RVE's heavy atom between the crystal conformation overlapped with the conformation after the redocking process<sup>33</sup>. For molecular dynamics, the analysis focused on assessing the stability of the salicylate synthase and compound complexes based on RMSD and RMSF criteria. The measurement of Rg was used to examine the protein folding during the simulation, which correlates with the complex's stability<sup>34</sup>. A lower SASA value indicates a more stable ligand-receptor complex. Lastly, the effectiveness of chemical constituents from *Xestospongia sp.* in binding with MTB salicylate synthase was assessed by calculating their binding energy using MM/GBSA approach.

## RESULTS AND DISCUSSION

### Molecular docking study

*Mycobacterium tuberculosis* remains a primary infectious disease with a high mortality rate in every country. Therefore, searching for compounds that can be candidates for anti-tuberculosis drugs is still very much needed. Computational studies using molecular docking methods are essential in accelerating drug development, especially in finding lead compounds<sup>35</sup>. This study tries to reveal the potential of *Xestospongia sp.* to inhibit mycobactin biosynthesis in MTB.

Based on the validation results, the redocking technique obtained an RMSD RVE value of 0.47 Å (**Figure 1**). This RMSD value was calculated by measuring the distance of RVE's heavy atom between the crystal conformation overlapped with the conformation after the redocking process. The best RVE conformation from the redocking results has a bond energy of -9.17 kcal/mol. This conformation's hydroxyl and carbonyl groups form hydrogen bonds with residues Gly270, Tyr385, Arg405, Gly419, Gly421, and Lys438 on the active site of MTB salicylate synthase<sup>19</sup>. In addition, the RVE benzene ring exhibits hydrophobic interactions with Leu268 and His334.

A total of 30 compounds from *Xestospongia sp.* gave a binding energy range from -0.15 to -9.98 kcal/mol, and as many as 16 compounds do not provide binding affinity. This binding affinity indicates the stability of the binding between the ligand and the target protein<sup>36</sup>. Two potential compounds from this marine sponge are CMNPD7640 (secoadociaquinone B) and CMNPD15071 (sulfuric acid mono-(8-methoxy-12b-methyl-6-oxo-2,3,6,12b-tetrahydro-1H-5-oxa-benzo [k]acephenanthrylen-11-yl) ester) (**Figure 2**) has a better binding affinity than RVE and binds to the active site of salicylate synthase with energies of -9.98 and -9.93 kcal/mol, respectively. In addition, these two compounds are also estimated to have an inhibition constant of 52.29 nM for CMNPD7640 and 48.59 nM for CMNPD15071.

Interestingly, these two compounds share a similar basic framework, being quinone derivatives, and exhibit a similar interaction pattern with RVE. The CMNPD7640 and CMNPD15071 compounds exhibit similar interactions, including hydrogen bonding with residues Lys205, Gly270, Thr271, His334, Glu431, and Lys438, as well as hydrophobic interactions with two residues Ala269 and Ile423 on the binding site of MTB salicylate synthase. Furthermore, unique hydrogen bonding was observed in the CMNPD7640 sulfonate groups that interacted with Arg405. Meanwhile, the sulfonate group of CMNPD15071 interacts with Ser301 (**Figure 2**). The 2D structure of the best-identified compound from *Xestospongia sp.* is depicted in **Figure 3**, as determined by molecular docking results.

### Molecular dynamics simulation

The stability of the top two hit compounds obtained from the molecular docking process was verified through a 50 ns MD simulation. The MD trajectory was utilized to compute the RMSD of the entire complex system<sup>37</sup> and the corresponding graph is depicted in **Figures 4A-C**. During the simulation, it was observed that the salicylate synthase complex with the RVE inhibitor exhibited the highest stability, as indicated by an average RMSD of 0.606 nm. When the salicylate synthase interacted with the compound CMNPD15071, it demonstrated even better stability than CMNPD7640, with average RMSD

values of 0.648 and 0.689 nm, respectively. Interestingly, the compound CMNPD15071 derived from *Xestospongia sp.* exhibited exceptional stability with a low RMSD of 0.163 nm. Moreover, the RVE inhibitor and CMNPD7640 also displayed reasonably stable interactions with RMSD average values of 0.179 and 0.325 nm, respectively.

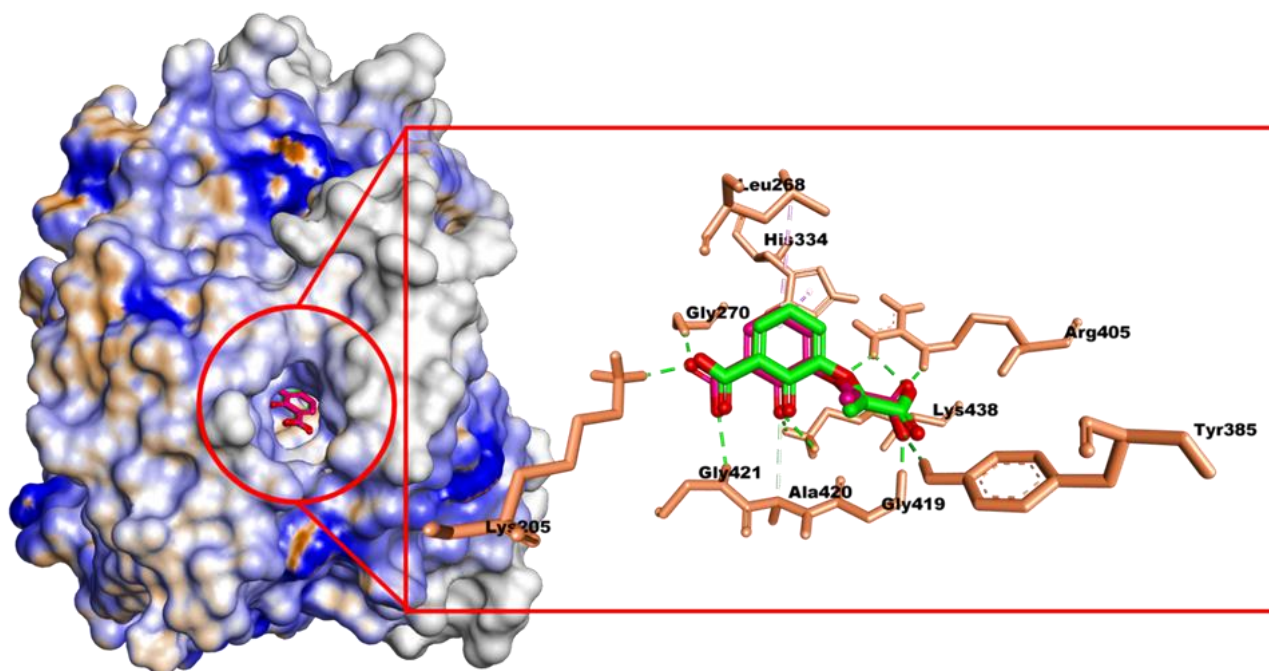


**Figure 1.** Visualization of the RVE crystallographic conformation (green) overlapping with the redocking conformation (pink) on the active site of MTB salicylate synthase. Dashed lines in green and pink indicate hydrogen bonds and hydrophobic interactions.

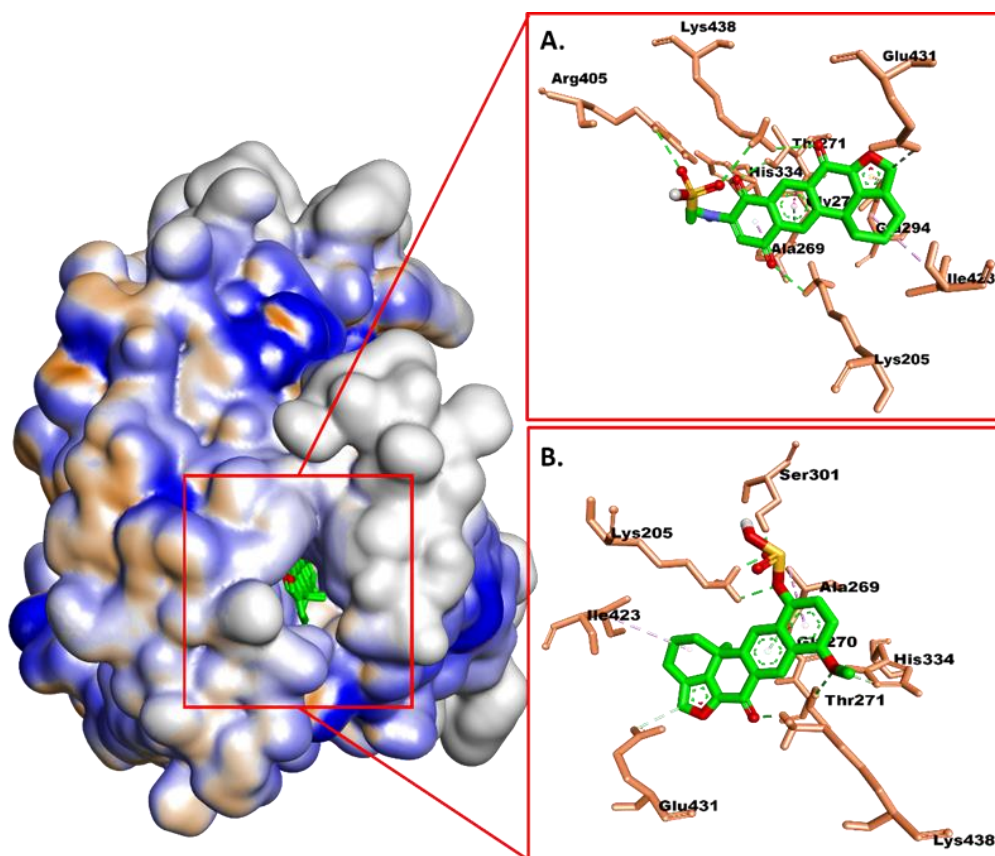


**Figure 2.** Molecular interactions of the best compounds from the *Xestospongia sp.* on the active site of the MTB salicylate synthase. (A) CMNPD7640 and (B) CMNPD15071.

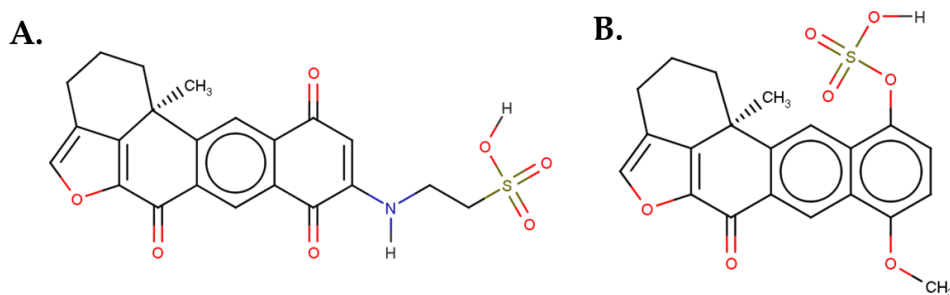


Figure 3. 2D structures representation of (A) CMNPD7640 and (B) CMNPD15071.

Meanwhile, during the simulation, the RMSF value for each complex was recorded, and the corresponding graph is shown in Figure 4D. This RMSF graph provides insights into the fluctuation of amino acid residues in the salicylate synthase over the 50 ns simulation period. Notably, all complexes exhibited a similar trend of fluctuating amino acid residues, with certain residues showing high-intensity oscillations. Specifically, residues Ala7, Pro278, Lys293, Ser331, and Gly412 displayed significant fluctuations. Notably, residues 293-304 demonstrated higher fluctuations than other compounds. However, the RMSF graph also highlighted a compelling observation: CMNPD15071 exhibited the ability to stabilize the amino acid residues of MTB salicylate synthase, resulting in lower fluctuations compared to other compounds. This finding suggests that CMNPD15071 may form more stable interactions with the salicylate synthase, potentially contributing to its inhibitory potential against MTB.

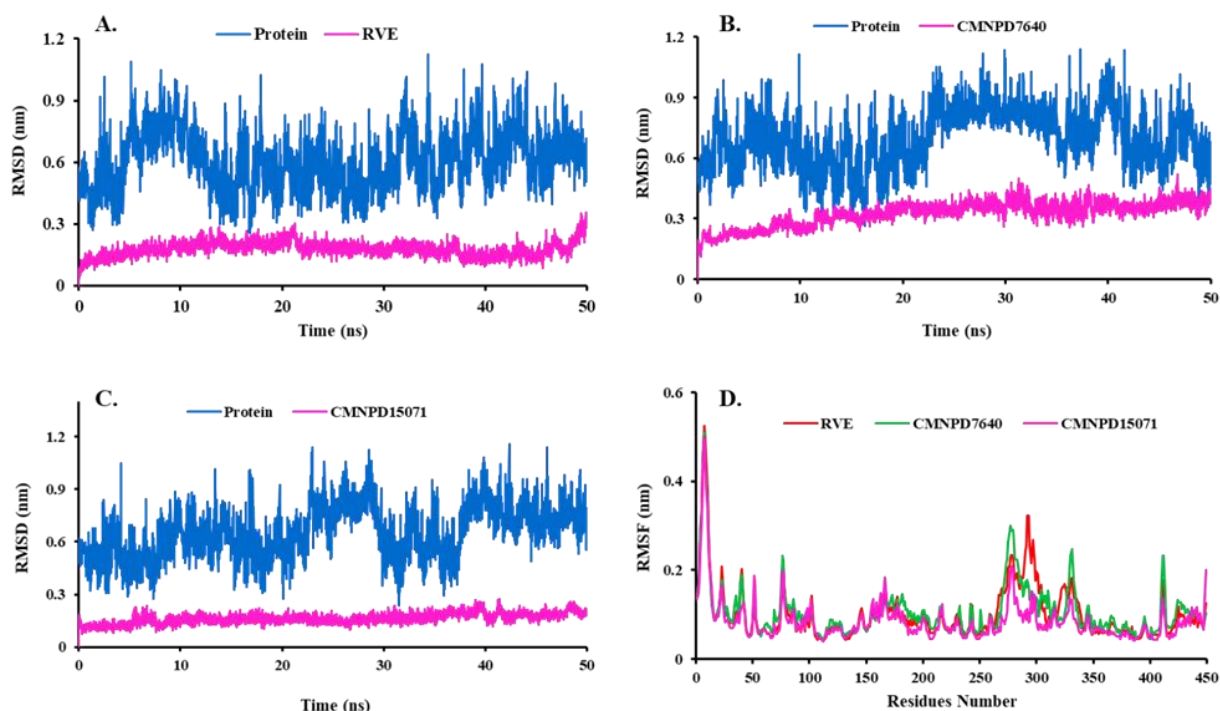


Figure 4. Evaluation of the RMSD criteria for the salicylate synthase-compounds complex of (A) protein-RVE, (B) protein-CMNPD7640, (C) protein-CMNPD15071, and (D) RMSF MTB salicylate synthase backbone during 50 ns MD simulation.

The plot of Rg is presented in Figure 5A. The lowest Rg value indicated the most stable compound in the complex with salicylate synthase. The best-hit compound was observed to have the same protein folding stability during the simulation<sup>38</sup>. Based on the analysis results, the average Rg values of the CMNPD15071 and CMNPD7640 complexes were 2.228 and 2.229 nm, respectively, lower than the RVE Rg value of 2.234 nm. These findings show that the CMNPD15071 complex has the lowest Rg value and higher cohesiveness than other hit compounds.

To comprehensively investigate the stability of each hit compound complex, we conducted a SASA analysis for each ligand. This analysis provides valuable insights into the complex's folding and stability<sup>39</sup> by monitoring variations in the protein solvent area during the simulation (Figure 5B). The SASA analysis graph revealed that all hit compounds exhibited a similarly wide range of areas accessed by solvent molecules. The average SASA values for each complex were 196.87, 195.24, and 194.15 nm<sup>2</sup> for RVE, CMNPD7640, and CMNPD15071, respectively. Interestingly, CMNPD15071 demonstrated exceptional stability compared to the other compounds, as evidenced by its SASA area remaining relatively unchanged throughout the experiment. This suggests that CMNPD15071 forms vigorous interactions with the salicylate synthase, enhancing its stability within the complex.

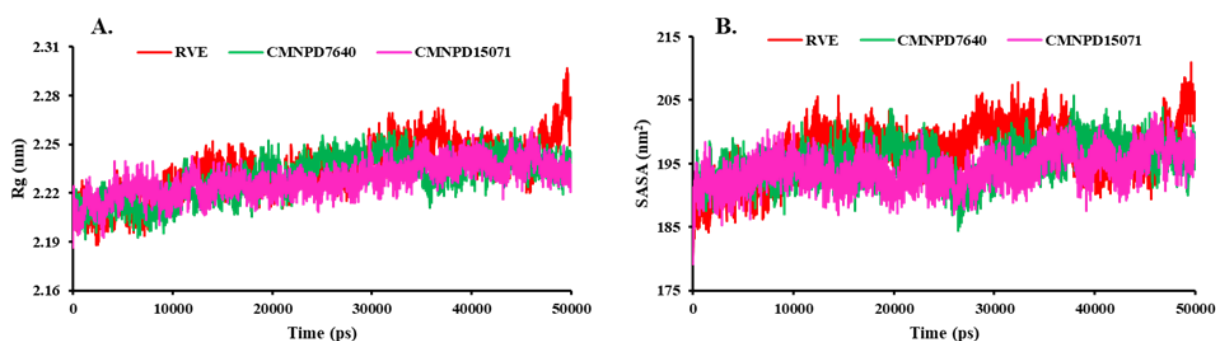


Figure 5. Evaluation of (A) Rg and (B) SASA graph during 50 ns MD simulations.

The effectiveness of chemical constituents from *Xestospongia sp.* in binding with MTB salicylate synthase was assessed by calculating their binding energy using the MM/GBSA approach. This influential computational tool delves into the molecular-level interactions between ligands and the receptor's active site, providing valuable insights into the stability and affinity of potential drug candidates as anti-TB agents<sup>40</sup>. The total binding energy ( $\Delta E_{\text{bind}}$ ) for the RVE system, which serves as a known inhibitor, was determined to be -35.36 kJ/mol. This value reflects the totality of various interactions, including electrostatic, van der Waals, and solvation energies, which contribute to the overall stability of the ligand-receptor complex<sup>41</sup>. Interestingly, the energy of CMNPD15071 was more negative at -38.48 kJ/mol, indicating that this compound may have a stronger binding affinity to MTB salicylate synthase than the RVE inhibitor, suggesting that it may form highly stable interactions with the target enzyme. On the other hand, CMNPD7640 exhibited a more positive binding energy of -26.03 J/mol than RVE. In Table I, we presented a comprehensive set of calculated binding energies for each system, providing a detailed comparison of the potential inhibitory capabilities of the compounds from *Xestospongia sp.* against MTB salicylate synthase.

To understand the molecular-level details, we analyzed the individual energy components contributing to the overall binding stability. The electrostatic energy ( $\Delta E_{\text{ELE}}$ ) arises from the electrostatic interactions between charged residues in the active site of MTB salicylate synthase and the ligand<sup>42</sup>. In the RVE system, this energy was slightly positive at 70.05 kJ/mol, suggesting a net repulsion between the ligand and the receptor. However, CMNPD15071 exhibited a significantly more negative value of -47.56 kJ/mol, indicating attractive electrostatic interactions with specific residues in the active site. Likewise, CMNPD7640 displayed a highly negative electrostatic energy of -74.75 kJ/mol, indicating strong attractive forces between the ligand and the enzyme. This result may be attributed to interactions formed by *Xestospongia sp.* compounds with positively charged residues of Lys205 and His334, as well as negatively charged Glu431, contributing to the electrostatic energy when binding to MTB salicylate synthase.

Conversely, the electrostatic contribution to the solvation energy ( $\Delta E_{\text{GB}}$ ) considers the interactions of the ligand with the solvent molecules in the surrounding environment<sup>43</sup>. The RVE system demonstrated a relatively negative value of -79.07 kJ/mol, indicating a favorable solvation effect that promotes binding. However, both CMNPD15071 and CMNPD7640 showed positive values (61.3 and 89.91 kJ/mol, respectively), suggesting that these compounds may experience less favorable solvation effects when binding to MTB salicylate synthase. Nevertheless, the positive solvation contribution does not negate their potential as inhibitors, as other strong interactions contribute to their overall binding affinity<sup>44</sup>.

Furthermore, the van der Waals energy ( $\Delta E_{\text{VDW}}$ ) was pivotal in the favorable binding energy<sup>45</sup>. CMNPD7640 and CMNPD15071 displayed highly negative van der Waals energies (-35.6 and -45.69 kJ/mol, respectively), indicating strong

attractive forces between the ligand and the enzyme's hydrophobic pockets. These values were significantly more negative than the RVE system's van der Waals energy (-22.33 kJ/mol), implying that the *Xestospongia sp.* compounds may form tighter and more stable interactions within the active site of MTB salicylate synthase.

**Table I.** The MM/GBSA binding energy calculated for the RVE and chemical constituents from *Xestospongia sp.*

Energies (kJ/mol)	RVE	CMNPD7640	CMNPD15071
$\Delta E_{VDW}$	-22.33	-35.60	-45.69
$\Delta E_{ELE}$	70.05	-74.75	-47.56
$\Delta E_{GB}$	-79.07	89.91	61.30
$\Delta E_{SURF}$	-4.01	-5.59	-6.53
$\Delta E_{Bind}$	-35.36	-26.03	-38.48

In summary, this comprehensive computational analysis provides valuable molecular insights into the potential inhibitory capabilities of chemical constituents from *Xestospongia sp.* against MTB salicylate synthase. The study highlights CMNPD15071 and CMNPD7640 as promising candidates for further investigation and development as potential therapeutic agents against tuberculosis. Moreover, these findings underscore the significant potential of marine natural products in the quest for novel anti-TB drugs, setting the stage for further experimental validations in drug development.

## CONCLUSION

This study succeeded in identifying CMNPD15071 (sulfuric acid mono-(8-methoxy-12b-methyl-6-oxo-2,3,6,12b-tetrahydro-1H-5-oxa-benzo[k]acephenanthrylen-11-yl) ester) and CMNPD7640 (secoadociaquinone B) from *Xestospongia sp.* which can inhibit mycobactin biosynthesis based on their affinity and interaction to MTB salicylate synthase. However, further research based on molecular dynamics studies showed that the CMNPD15071 has the potential as a lead compound for the salicylate synthase inhibitor of MTB. This finding can be an impetus for future investigations for antimicrobial agents against MTB.

## ACKNOWLEDGMENT

The authors would like to thank the facilities and research support provided by the Faculty of Pharmacy, Universitas Halu Oleo, Kendari, Southeast Sulawesi, Indonesia.

## AUTHORS' CONTRIBUTION

**Conceptualization:** Arfan, Aiyi Asnawi, La Ode Aman

**Data curation:** Arfan

**Formal analysis:** Arfan

**Funding acquisition:** Arfan, Aiyi Asnawi, La Ode Aman

**Investigation:** Arfan, Aiyi Asnawi, La Ode Aman

**Methodology:** Aiyi Asnawi, La Ode Aman

**Project administration:** Arfan, Aiyi Asnawi, La Ode Aman

**Resources:** Aiyi Asnawi, La Ode Aman

**Software:** Aiyi Asnawi, La Ode Aman

**Supervision:** Aiyi Asnawi, La Ode Aman

**Validation:** Arfan

**Visualization:** Arfan

**Writing - original draft:** Arfan, Aiyi Asnawi, La Ode Aman

**Writing - review & editing:** Arfan, Aiyi Asnawi, La Ode Aman

## DATA AVAILABILITY

All data related to this study are included herein.

## CONFLICT OF INTEREST

The authors declare no conflict of interest.

## REFERENCES

1. Pavlik I, Ulmann V, Hubelova D, Weston RT. Nontuberculous Mycobacteria as Saprophytes: A Review. *Microorganisms*. 2022;(10):1345–57. DOI: [10.3390/microorganisms10071345](https://doi.org/10.3390/microorganisms10071345); PMCID: [PMC9315685](https://pubmed.ncbi.nlm.nih.gov/35889064/); PMID: [35889064](https://pubmed.ncbi.nlm.nih.gov/35889064/)
2. Delghandi MR, El-Matbouli M, Menanteau-Ledouble S. Mycobacteriosis and Infections with Non-tuberculous Mycobacteria in Aquatic Organisms: A Review. *Microorganisms*. 2020;(8):1368–86. DOI: [10.3390/microorganisms8091368](https://doi.org/10.3390/microorganisms8091368); PMCID: [PMC7564596](https://pubmed.ncbi.nlm.nih.gov/32906655/); PMID: [32906655](https://pubmed.ncbi.nlm.nih.gov/32906655/)
3. Chandra P, Grigsby SJ, Philips JA. Immune evasion and provocation by *Mycobacterium tuberculosis*. *Nat Rev Microbiol*. 2022;20(12):750–66. DOI: [10.1038/s41579-022-00763-4](https://doi.org/10.1038/s41579-022-00763-4); PMCID: [PMC9310001](https://pubmed.ncbi.nlm.nih.gov/35879556/); PMID: [35879556](https://pubmed.ncbi.nlm.nih.gov/35879556/)
4. Pai M, Behr MA, Dowdy D, Dheda K, Divangahi M, Boehme CC, Ginsberg A, et al. Tuberculosis. *Nat Rev Dis Prim*. 2016;2:16076. DOI: [10.1038/nrdp.2016.76](https://doi.org/10.1038/nrdp.2016.76); PMID: [27784885](https://pubmed.ncbi.nlm.nih.gov/27784885/)
5. Avoi R, Liaw YC. Tuberculosis Death Epidemiology and Its Associated Risk Factors in Sabah, Malaysia. *Int J of Envir Res and Pub*. 2021;18(18):9740. DOI: [10.3390/ijerph18189740](https://doi.org/10.3390/ijerph18189740); PMCID: [PMC8470141](https://pubmed.ncbi.nlm.nih.gov/34574665/); PMID: [34574665](https://pubmed.ncbi.nlm.nih.gov/34574665/)
6. Seung KJ, Keshavjee S, Rich ML. Multidrug-Resistant Tuberculosis and Extensively Drug-Resistant Tuberculosis. *Cold Spring Harb Perspect Med*. 2015;5(9):a017863. DOI: [10.1101/cshperspect.a017863](https://doi.org/10.1101/cshperspect.a017863); PMCID: [PMC4561400](https://pubmed.ncbi.nlm.nih.gov/25918181/); PMID: [25918181](https://pubmed.ncbi.nlm.nih.gov/25918181/)
7. Miethke M, Pieroni M, Weber T, Brönstrup M, Hammann P, Halby L, et al. Towards the sustainable discovery and development of new antibiotics. *Nat Rev Chem*. 2021;5(10):726–49. DOI: [10.1038/s41570-021-00313-1](https://doi.org/10.1038/s41570-021-00313-1); PMCID: [PMC8374425](https://pubmed.ncbi.nlm.nih.gov/34426795/); PMID: [34426795](https://pubmed.ncbi.nlm.nih.gov/34426795/)
8. Mori M, Stelitano G, Griego A, Chiarelli LR, Cazzaniga G, Gelain A, et al. Synthesis and Assessment of the In Vitro and Ex Vivo Activity of Salicylate Synthase (MbtI) Inhibitors as New Candidates for the Treatment of Mycobacterial Infections. *Pharmaceuticals*. 2022;15(8):992–1012. DOI: [10.3390/ph15080992](https://doi.org/10.3390/ph15080992); PMCID: [PMC9413995](https://pubmed.ncbi.nlm.nih.gov/36015139/); PMID: [36015139](https://pubmed.ncbi.nlm.nih.gov/36015139/)
9. Liu Z, Liu F, Aldrich CC. Stereocontrolled Synthesis of a Potential Transition-State Inhibitor of the Salicylate Synthase MbtI from *Mycobacterium tuberculosis*. *J Org Chem*. 2015;80(13):6545–52. DOI: [10.1021/acs.joc.5b00455](https://doi.org/10.1021/acs.joc.5b00455); PMCID: [PMC4667787](https://pubmed.ncbi.nlm.nih.gov/26035083/); PMID: [26035083](https://pubmed.ncbi.nlm.nih.gov/26035083/)
10. Zhang L, Hendrickson RC, Meikle V, Lefkowitz EJ, Ioerger TR, Niederweis M. Comprehensive analysis of iron utilization by *Mycobacterium tuberculosis*. *PLOS Pathog*. 2020;16(2):e1008337. DOI: [10.1371/journal.ppat.1008337](https://doi.org/10.1371/journal.ppat.1008337); PMCID: [PMC7058343](https://pubmed.ncbi.nlm.nih.gov/32069330/); PMID: [32069330](https://pubmed.ncbi.nlm.nih.gov/32069330/)
11. Cloete R, Oppon E, Murungi E, Schubert WD, Christoffels A. Resistance related metabolic pathways for drug target identification in *Mycobacterium tuberculosis*. *BMC Bioinformatics*. 2016;17:75. DOI: [10.1186/s12859-016-0898-8](https://doi.org/10.1186/s12859-016-0898-8); PMCID: [PMC4745158](https://pubmed.ncbi.nlm.nih.gov/26856535/); PMID: [26856535](https://pubmed.ncbi.nlm.nih.gov/26856535/)
12. Chiarelli LR, Mori M, Barlocco D, Beretta G, Gelain A, Pini E, et al. Discovery and development of novel salicylate synthase (MbtI) furanic inhibitors as antitubercular agents. *Eur J Med Chem*. 2018;155:754–63. DOI: [10.1016/j.ejmech.2018.06.033](https://doi.org/10.1016/j.ejmech.2018.06.033); PMID: [29940465](https://pubmed.ncbi.nlm.nih.gov/29940465/)

13. Chiarelli LR, Mori M, Beretta G, Gelain A, Pini E, Sammartino JC, et al. New insight into structure-activity of furan-based salicylate synthase (MbtI) inhibitors as potential antitubercular agents. *J Enzyme Inhib Med Chem*. 2019;34(1):823–8. DOI: [10.1080/14756366.2019.1589462](https://doi.org/10.1080/14756366.2019.1589462); PMCID: [PMC6427685](https://pubmed.ncbi.nlm.nih.gov/30889995/); PMID: 30889995
14. Pini E, Poli G, Tuccinardi T, Chiarelli LR, Mori M, Gelain A, et al. New Chromane-Based Derivatives as Inhibitors of Mycobacterium tuberculosis Salicylate Synthase (MbtI): Preliminary Biological Evaluation and Molecular Modeling Studies. *Molecules*. 2018;23(7):1506. DOI: [10.3390/molecules23071506](https://doi.org/10.3390/molecules23071506); PMCID: [PMC6099841](https://pubmed.ncbi.nlm.nih.gov/29933627/); PMID: 29933627
15. Karthikeyan A, Joseph A, Nair BG. Promising bioactive compounds from the marine environment and their potential effects on various diseases. *J Genet Eng Biotechnol*. 2022;20(1):14. DOI: [10.1186/s43141-021-00290-4](https://doi.org/10.1186/s43141-021-00290-4); PMCID: [PMC8790952](https://pubmed.ncbi.nlm.nih.gov/35080679/); PMID: 35080679
16. Pujiastuti DY, Amin MNG, Alamsjah MA, Hsu JL. Marine Organisms as Potential Sources of Bioactive Peptides that Inhibit the Activity of Angiotensin I-Converting Enzyme: A Review. *Molecules*. 2019;(24):2541. DOI: [10.3390/molecules24142541](https://doi.org/10.3390/molecules24142541); PMCID: [PMC6680877](https://pubmed.ncbi.nlm.nih.gov/31336853/); PMID: 31336853
17. Yamazaki H. Exploration of marine natural resources in Indonesia and development of efficient strategies for the production of microbial halogenated metabolites. *J Nat Med*. 2022;76(1):1–19. DOI: [10.1007/s11418-021-01557-3](https://doi.org/10.1007/s11418-021-01557-3); PMCID: [PMC8732978](https://pubmed.ncbi.nlm.nih.gov/34415546/); PMID: 34415546
18. Swantara MD, Rita WS, Suartha N, Agustina KK. Anticancer activities of toxic isolate of Xestospongia testudinaria sponge. *Vet World*. 2019;12(9):1434–40. DOI: [10.14202/vetworld.2019.1434-1440](https://doi.org/10.14202/vetworld.2019.1434-1440); PMCID: [PMC6813599](https://pubmed.ncbi.nlm.nih.gov/31749578/); PMID: 31749578
19. Chi G, Manos-Turvey A, O'Connor PD, Johnston JM, Evans GL, Baker EN, et al. Implications of Binding Mode and Active Site Flexibility for Inhibitor Potency against the Salicylate Synthase from Mycobacterium tuberculosis. *Biochemistry*. 2012;51(24):4868–79. DOI: [10.1021/bi3002067](https://doi.org/10.1021/bi3002067); PMID: 22607697
20. Arba M, Arfan, Trisnawati A, Kurniawati D. Pemodelan Farmakofor untuk Identifikasi Inhibitor Heat Shock Proteins-90 (HSP-90). *J Farmasi Galenika Galenika J Pharm*. 2020;6(2):229–36. DOI: [10.22487/j24428744.2020.v6.i2.15036](https://doi.org/10.22487/j24428744.2020.v6.i2.15036)
21. Morris GM, Huey R, Lindstrom W, Sanner MF, Belew RK, Goodsell DS, et al. AutoDock4 and AutoDockTools4: Automated Docking with Selective Receptor Flexibility. *J Comput Chem*. 2009;30(16):2785–91. DOI: [10.1002/jcc.21256](https://doi.org/10.1002/jcc.21256); PMCID: [PMC2760638](https://pubmed.ncbi.nlm.nih.gov/19399780/); PMID: 19399780
22. Lyu C, Chen T, Qiang B, Liu N, Wang H, Zhang L, Liu Z. CMNPD: a comprehensive marine natural products database towards facilitating drug discovery from the ocean. *Nucleic Acids Res*. 2021;49(D1):D509–15. DOI: [10.1093/nar/gkaa763](https://doi.org/10.1093/nar/gkaa763); PMCID: [PMC7779072](https://pubmed.ncbi.nlm.nih.gov/32986829/); PMID: 32986829
23. O'Boyle NM, Banck M, James CA, Morley C, Vandermeersch T, Hutchison GR. Open Babel: An open chemical toolbox. *J Cheminform*. 2011;3:33. DOI: [10.1186/1758-2946-3-33](https://doi.org/10.1186/1758-2946-3-33); PMCID: [PMC3198950](https://pubmed.ncbi.nlm.nih.gov/21982300/); PMID: 21982300
24. Morris GM, Huey R, Olson AJ. Using AutoDock for ligand-receptor docking. *Curr Protoc Bioinformatics*. 2008;Ch8:Unit 8.14 DOI: [10.1002/0471250953.bi0814s24](https://doi.org/10.1002/0471250953.bi0814s24); PMID: 19085980
25. Arfan A, Muliadi R, Malina R, Trinovitasari N, Asnawi A. Docking and Dynamics Studies: Identifying the Binding Ability of Quercetin Analogs to the ADP-Ribose Phosphatase of SARS CoV-2. *J Kartika Kimia*. 2022;5(2):145–51. DOI: [10.26874/jkk.v5i2.143](https://doi.org/10.26874/jkk.v5i2.143)
26. Kohnke B, Kutzner C, Grubmüller H. A GPU-Accelerated Fast Multipole Method for GROMACS: Performance and Accuracy. *J Chem Theory Comput*. 2020;16(11):6938–49. DOI: [10.1021/acs.jctc.0c00744](https://doi.org/10.1021/acs.jctc.0c00744); PMCID: [PMC7660746](https://pubmed.ncbi.nlm.nih.gov/33084336/); PMID: 33084336
27. Petrov D, Zagrovic B. Are current atomistic force fields accurate enough to study proteins in crowded environments? *PLoS Comput Biol*. 2014;10(5):e1003638. DOI: [10.1371/journal.pcbi.1003638](https://doi.org/10.1371/journal.pcbi.1003638); PMCID: [PMC4031056](https://pubmed.ncbi.nlm.nih.gov/24854339/); PMID: 24854339

28. Wang J, Wolf RM, Caldwell JW, Kollman PA, Case DA. Development and testing of a general amber force field. *J Comput Chem.* 2004;25(9):1157-74. DOI: [10.1002/jcc.20035](https://doi.org/10.1002/jcc.20035); PMID: [15116359](https://pubmed.ncbi.nlm.nih.gov/15116359/)
29. da Silva AWS, Vranken WF. ACPYPE - AnteChamber PYthon Parser interfacE. *BMC Res Notes.* 2012;5(367):367. DOI: [10.1186/1756-0500-5-367](https://doi.org/10.1186/1756-0500-5-367); PMCID: [PMC3461484](https://pubmed.ncbi.nlm.nih.gov/PMC3461484/); PMID: [22824207](https://pubmed.ncbi.nlm.nih.gov/22824207/)
30. Asnawi A, Febrina E, Aligita W, Yuliantini A, Arfan A. Penambatan Molekul dan Dinamika Molekul beberapa Fitokimia dari *Acalypha Indica* L. sebagai Inhibitor Matriks Metalloproteinase<sup>9</sup>. *J Sains Farmasi Klinis.* 2023;10(1):69-77. DOI: [10.25077/jsfk.10.1.69-77.2023](https://doi.org/10.25077/jsfk.10.1.69-77.2023)
31. Aman LO, Sihalo M, Arfan A. Pencarian Inhibitor DYRK2 dari Database Bahan Alam Zinc<sup>15</sup>: Analisis Farmakofor, Simulasi Docking dan Dinamika Molekuler. *J Sains Farmasi Klinis.* 2023;10(1):100-13. DOI: [10.25077/jsfk.10.1.100-113.2023](https://doi.org/10.25077/jsfk.10.1.100-113.2023)
32. Asnawi A, Aman LO, Yuliantini A, Febrina E. Molecular Docking and Molecular Dynamic Studies: Screening Phytochemicals of *Acalypha Indica* against Braf Kinase Receptors for Potential use in Melanocytic Tumours. *Rasayan J Chem.* 2022;15(2):1352-61. DOI: [10.31788/RJC.2022.1526769](https://doi.org/10.31788/RJC.2022.1526769)
33. Meng XY, Zhang HX, Mezei M, Cui M. Molecular docking: a powerful approach for structure-based drug discovery. *Curr Comput Aided Drug Des.* 2011;7(2):146-57. DOI: [10.2174/157340911795677602](https://doi.org/10.2174/157340911795677602); PMCID: [PMC3151162](https://pubmed.ncbi.nlm.nih.gov/PMC3151162/); PMID: [21534921](https://pubmed.ncbi.nlm.nih.gov/21534921/)
34. Rampogu S, Lee G, Park JS, Lee KW, Kim MO. Molecular Docking and Molecular Dynamics Simulations Discover Curcumin Analogue as a Plausible Dual Inhibitor for SARS-CoV-2. *Int J Mol Sci.* 2022;23(3):1771. DOI: [10.3390/ijms23031771](https://doi.org/10.3390/ijms23031771); PMCID: [PMC8836015](https://pubmed.ncbi.nlm.nih.gov/PMC8836015/); PMID: [35163692](https://pubmed.ncbi.nlm.nih.gov/35163692/)
35. Citra SNAL, Arfan A, Alroem A, Bande LS, Irnawati I, Arba M. Docking-based workflow and ADME prediction of some compounds in *Curcuma longa* and *Andrographis paniculata* as polymerase PA-PB1 inhibitors of influenza A/H5N1 virus. *J Res Pharm.* 2023;27(1):221-31. DOI: [10.29228/jrp.305](https://doi.org/10.29228/jrp.305)
36. Du X, Li Y, Xia YL, Ai SM, Liang J, Sang P, et al. Insights into Protein-Ligand Interactions: Mechanisms, Models, and Methods. *Int J Mol Sci.* 2016;17(2):144. DOI: [10.3390/ijms17020144](https://doi.org/10.3390/ijms17020144); PMCID: [PMC4783878](https://pubmed.ncbi.nlm.nih.gov/PMC4783878/); PMID: [26821017](https://pubmed.ncbi.nlm.nih.gov/26821017/)
37. Ghahremanian S, Rashidi MM, Raeisi K, Toghraie D. Molecular dynamics simulation approach for discovering potential inhibitors against SARS-CoV-2: A structural review. *J Mol Liq.* 2022;354:118901. DOI: [10.1016/j.molliq.2022.118901](https://doi.org/10.1016/j.molliq.2022.118901); PMCID: [PMC8916543](https://pubmed.ncbi.nlm.nih.gov/PMC8916543/); PMID: [35309259](https://pubmed.ncbi.nlm.nih.gov/35309259/)
38. Rakhsit G, Biswas A, Jayaprakash V. In Silico Drug Repurposing Studies for the Discovery of Novel Salicyl-AMP Ligase (MbtA) Inhibitors. *Pathogens.* 2023;12(12):1433. DOI: [10.3390/pathogens12121433](https://doi.org/10.3390/pathogens12121433); PMCID: [PMC10745912](https://pubmed.ncbi.nlm.nih.gov/PMC10745912/); PMID: [38133316](https://pubmed.ncbi.nlm.nih.gov/38133316/)
39. Ali SA, Hassan MI, Islam A, Ahmad F. A review of methods available to estimate solvent-accessible surface areas of soluble proteins in the folded and unfolded states. *Curr Protein Pept Sci.* 2014;15(5):456-76. DOI: [10.2174/1389203715666140327114232](https://doi.org/10.2174/1389203715666140327114232); PMID: [24678666](https://pubmed.ncbi.nlm.nih.gov/24678666/)
40. Genheden S, Ryde U. The MM/PBSA and MM/GBSA methods to estimate ligand-binding affinities. *Expert Opin Drug Discov.* 2015;10(5):449-61. DOI: [10.1517/17460441.2015.1032936](https://doi.org/10.1517/17460441.2015.1032936); PMCID: [PMC4487606](https://pubmed.ncbi.nlm.nih.gov/PMC4487606/); PMID: [25835573](https://pubmed.ncbi.nlm.nih.gov/25835573/)
41. Li Z, Chan KC, Nickels JD, Cheng X. Electrostatic Contributions to the Binding Free Energy of Nicotine to the Acetylcholine Binding Protein. *J Phys Chem B.* 2022;126(43):8669-79. DOI: [10.1021/acs.jpcc.2c04641](https://doi.org/10.1021/acs.jpcc.2c04641); PMCID: [PMC10056799](https://pubmed.ncbi.nlm.nih.gov/PMC10056799/); PMID: [36260486](https://pubmed.ncbi.nlm.nih.gov/36260486/)
42. Arfan A, Muliadi R, Rayani R. Eksplorasi Senyawa Penghambat Enzim Salisilat Sintase dari *Mycobacterium tuberculosis* melalui Studi Penambatan Molekul dan Prediksi Sifat ADME. *Lansau J Ilmu Kefarmasian.* 2023;1(1):77-88. DOI: [10.33772/lansau.v1i1.9](https://doi.org/10.33772/lansau.v1i1.9)

43. Izadi S, Aguilar B, Onufriev AV. Protein-Ligand Electrostatic Binding Free Energies from Explicit and Implicit Solvation. *J Chem Theory Comput.* 2015;11(9):4450-9. DOI: [10.1021/acs.jctc.5b00483](https://doi.org/10.1021/acs.jctc.5b00483); PMCID: [PMC5217485](https://pubmed.ncbi.nlm.nih.gov/26575935/); PMID: [26575935](https://pubmed.ncbi.nlm.nih.gov/26575935/)
44. Pansar T, Poso A. Binding Affinity via Docking: Fact and Fiction. *Molecules.* 2018;23(8):1899. DOI: [10.3390/molecules23081899](https://doi.org/10.3390/molecules23081899); PMCID: [PMC6222344](https://pubmed.ncbi.nlm.nih.gov/30061498/); PMID: [30061498](https://pubmed.ncbi.nlm.nih.gov/30061498/)
45. Roth CM, Neal BL, Lenhoff AM. Van der Waals interactions involving proteins. *Biophys J.* 1996;70(2):977-87. DOI: [10.1016/s0006-3495\(96\)79641-8](https://doi.org/10.1016/s0006-3495(96)79641-8); PMCID: [PMC1224998](https://pubmed.ncbi.nlm.nih.gov/8789115/); PMID: [8789115](https://pubmed.ncbi.nlm.nih.gov/8789115/)